

THE PENNSYLVANIA STATE UNIVERSITY
SCHREYER HONORS COLLEGE

DEPARTMENT OF MATHEMATICS

GEOSPATIAL-RISK-BASED RECOUPMENT FOR TRIA-ELIGIBLE INSURANCE

RAFAEL BERGERMAN
SPRING 2019

A thesis
submitted in partial fulfillment
of the requirements
for a baccalaureate degree
in Mathematics
with honors in Mathematics

Reviewed and approved* by the following:

Zhongyi Yuan
Assistant Professor of Risk Management
Thesis Supervisor

Sergei Tabachnikov
Professor of Mathematics
Honors Advisor

*Signatures are on file in the Schreyer Honors College.

Abstract

Terrorism risk has become a major threat to human lives and businesses around the world. In an effort to make insurance against such risk available and affordable in the United States, the Terrorism Risk Insurance Act (TRIA) was passed in 2002 to establish a public-private partnership and to provide subsidies for insuring terrorism losses. Essentially, under TRIA, government subsidies apply only to the insured losses above the market retention level. For those below the retention level, the government will recoup any claim payments it initially shares plus a 40% surcharge. The loss-sharing mechanism has been running untested for the past decade. The specification of its recoupment process has never been clear and remains a challenge. We propose an easily implemented recoupment scheme based on the geospatial risk of terrorist attacks. We use a geospatial point process to model terrorism risk and its occurrences, estimated using the Global Terrorism Database, and also illustrate our suggested recoupment for a hypothetical insurance portfolio.

Table of Contents

List of Figures	iii
List of Tables	iv
Acknowledgements	v
1 Introduction	1
1.1 TRIA	2
1.2 Loss Sharing Structure	3
1.3 Recoupment	5
1.4 Literature Review	6
1.5 Structure of the Paper	6
2 Model, Theory, and Proposal	8
2.1 Insurance Market	9
2.2 A Geospatial Framework for Terrorism Risk	10
2.3 Proposed Recoupment Scheme	11
3 Data	14
3.1 Global Terrorism Database	15
4 Empirical Studies	17
4.1 Data Analysis and Model Estimation	18
4.2 Inhomogeneous K-function	18
4.3 Inhomogeneous Pair Correlation Function	21
4.4 Our Model	23
4.5 Suggested Recoupment for a Hypothetical Portfolio	24
5 Concluding Remarks	27
5.1 Conclusion	28
Appendices	29
Appendix A	30
Appendix B	31
Bibliography	32

List of Figures

1.1	TRIA Loss Sharing Structure	4
1.2	TRIA Recoupment Mechanism.	5
3.1	Map of Terrorist Attacks 1970-2016	16
4.1	Inhomogeneous K-function Analysis	20
4.2	Inhomogeneous PCF Analysis	22
4.3	Estimated Intensities	23

List of Tables

2.1	A simple example to illustrate recoupment ideas	11
4.3	Annualized intensities for notable cities	24
4.4	A simple example to illustrate hypothetical recoupments	25
4.5	A simple example to illustrate hypothetical recoupments, continued	25
4.6	A simple example to illustrate hypothetical recoupments, continued	26
1	Number of Attacks by State, 1970-2016	30

Acknowledgements

To my family, Marcel, Maria, and Felipe for their unwavering support. To my friends for always providing inspiration. Thanks to my thesis supervisor Zhongyi Yuan for all the opportunities he gave me to succeed in our research.

Chapter 1

Introduction

1.1 TRIA

Terrorism, defined by an attack's intention of coercing or intimidating a large body of individuals, is a dynamic and ever-changing risk facing all nations worldwide. Since the turn of the decade, the world has experienced nearly 87,000 terrorism events¹, multiple of which have led to catastrophic property damages exceeding \$1 billion. For the year 2016 alone, there were 34,871 lives lost to terrorist attacks globally. Beyond the many tragic losses of life, terrorist attacks are known to disturb the financial markets (Chesney et al. 2011) and more so the insurance industry. For example, the most prominent of such events occurred on September 11th, 2001 as multiple U.S. targets were attacked by hijacked airplanes and resulted in an insured loss of over \$45 billion².

The catastrophic losses caused great concerns among insurers, who then began excluding terrorism coverage from their commercial policies. Coverage thus became scarce and when available, far too expensive. This response by the private insurance industry left many corporations uninsured from terrorism risk, forcing the U.S. Congress to intervene. The Terrorism Risk Insurance Act (TRIA) was passed in 2002 to establish a public-private partnership for sharing terrorism losses, with the government acting as a reinsurer for the private industry. In return for this protective layer, insurance companies must offer terrorism coverage to all policyholders on the same terms that are offered for other perils. U.S. companies are not mandated to purchase terrorism coverage unless required by state law, as is the case for Workers Compensation insurance in a majority of states. TRIA allows terrorism insurance to be purchased as a separate policy from the business's commercial policy, or purchased along with TRIA-eligible lines, such as fire, commercial multi-peril, and worker's compensation³.

So far, TRIA has been amended on three occasions with the most recent being in 2015. The program is due to expire in 2020 unless Congress once again renews the act. At the latest renewal, TRIA passed with strong bipartisan support. However, there is a small risk that TRIA will be used as a bargaining chip for passing other policies, potentially leading to its end.

Additionally, the current version of TRIA still presents multiple challenges for lawmakers. One such challenge is the creation of a pricing scheme to help the Treasury pay for future terrorism outlays. Since losses are shared between insurers and the government, a premium-like federal charge has been considered as an alternative solution to the current recoupment scheme. Such a charge would aid the government in paying for large terrorism losses. Another challenge is the lack of structure surrounding the aforementioned federally mandated recoupment on commercial policyholders. The regulation of the Terrorism Risk Insurance Program (TRIP) requires this recoupment surcharge to be a percentage of the premium charged on TRIA eligible lines (U.S. Treasury 2015), but there are no clear guidelines as to how exactly the percentage should be set. Currently, the Treasury does not have a plan or single methodology for determining a recoupment surcharge. The only guideline available is that the Treasury may take a few risk factors into consideration for their recoupment process, but no further instruction is offered about what those factors should be or will be. Moreover, they may need to issue data calls from the insurers to evaluate the risk factors, which may substantially delay the recoupment process. See U.S. Treasury (2018) for more details.

¹260 of which took place on United States soil.

²See <https://www.iii.org/article/background-on-terrorism-risk-and-insurance>.

³A more comprehensive list of TRIA-eligible lines can be found in a recent data call issued by the U.S. insurance regulators and the Treasury; see https://www.naic.org/industry_terrorism_risk_data_call.htm

The main contribution of our paper is a proposal of a recoupment scheme that reflects the geospatial risk of terrorism events and is easy to implement. Our scheme also facilitates timely recoupment, in the sense that the data required to estimate the quantities are already available to the regulators and/or Treasury, either from the previous year's report filings, or from data calls that can be completed earlier; no data call for the most recent data is required for implementation. By offering a geospatial terrorism risk model, our recoupment scheme can also serve as an important first step towards pricing terrorism (re)insurance – the other challenge facing the Treasury. It is our hope that addressing these challenges could help the decision-making on TRIA renewal in 2020.

1.2 Loss Sharing Structure

To demonstrate the current loss-sharing scheme, we first review the official government criteria for a terrorist attack then detail the current structure of TRIA. We then follow through a simple example.

Acts of terrorism in the U.S. must be certified by the Secretary of the Treasury as an event that satisfies the following criteria (U.S. Treasury 2015): the attack must be considered an “act of terrorism;” must be violent or dangerous to human life, property, or infrastructure; must take place within either the U.S., a U.S. air carrier, an American vessel, or on the premises of a U.S. mission; and must be committed by an individual or individuals, as part of an effort to coerce the civilian population of the U.S. or to influence the policy or affect the conduct of the United States Government by coercion. Additionally, acts are not eligible for certification if the attack is committed as a part of war officially declared by Congress (with the exception of Workers Compensation), or the aggregate property and casualty losses do not exceed \$5 million.

All terrorism events have to go through the certification process before TRIA-eligible insurance payments can be made. An important implication of this is that the government has first-hand complete information about the frequency of all such events that occurred in the past and some information about the loss severity. The government knows whether the losses from each terrorism event exceeded \$5 million, although the losses below the insurers' TRIA deductibles might not be reported.

The loss sharing structure described below only applies for certified acts of terrorism, and it is only triggered once aggregate losses over a calendar year exceed the program trigger, which is set to \$180 million in 2019⁴. The program is subsequently capped once aggregate losses reach \$100 billion. The part below \$100 billion is split as follows: the first layer is covered by policyholders in the form of policy deductibles. Above that is the layer covered by commercial insurance companies, each paying up to the firm's TRIA deductible, which is equal to 20% of the firm's direct earned premium (DEP) in the prior year. The final layer is shared between commercial insurers and the government, in which the latter covers 81%⁵ of losses above each company's TRIA deductible. The general structure of the loss-sharing can be seen in Figure 1.1.

⁴Program trigger at the 2015 renewal was set at \$100 million, increasing by \$20 million per year until hitting \$200 million in 2020.

⁵TRIA's 2015 renewal states that the government will pay 85% of losses above a firm's TRIA deductible, decreasing by 1% each year until hitting 80% in 2020.

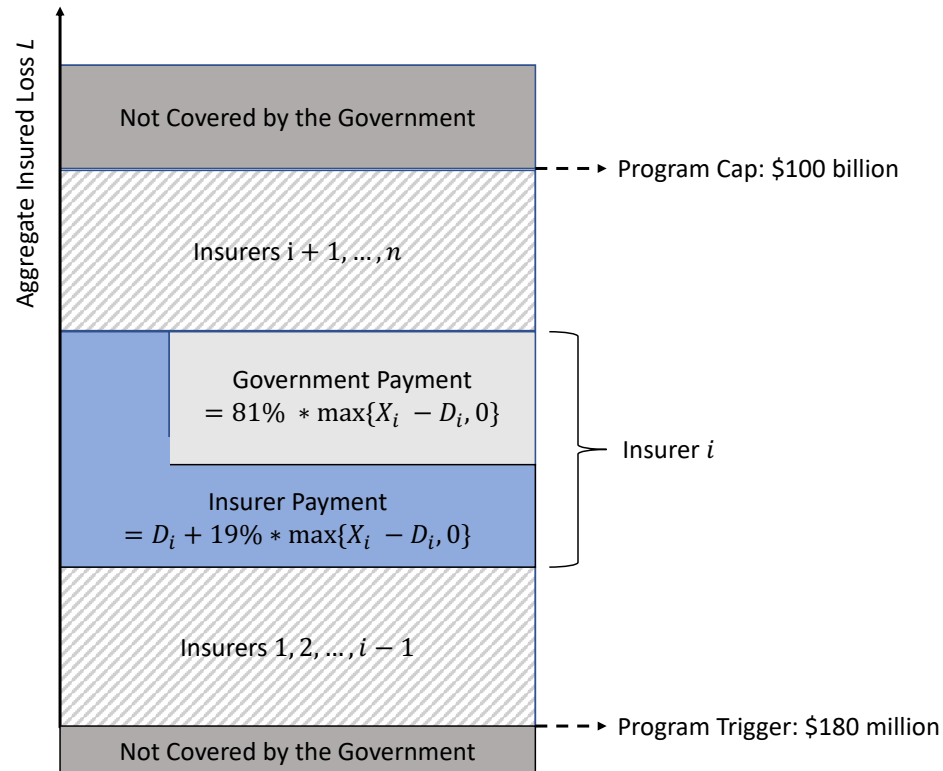


Figure 1.1: TRIA Loss Sharing Structure. This graph shows the loss sharing between policyholders, the insurers, and the federal government. Here D_i is Insurer i 's TRIA deductible, equal to 20% of its prior year DEP, and X_i is insurer i 's insurance payout. The government share of 81% applies for the year 2019. It has been decreasing by 1% over the years since 2015 and is set to decrease by another 1% in 2020. See U.S. Treasury (2018) and Michel-Kerjan and Kunreuther (2018) for similar illustrations.

If aggregate insured losses exceed the calendar year \$100 billion cap, the Secretary of the Treasury determines the proportionate share of losses to be paid out by each insurer that has incurred TRIA-eligible losses. The Treasury currently has no set method for determining the pro rata loss percentage (PRLP), although it does set some guidelines on which factors may be considered. These include estimates of insured losses from both statistical organizations and data calls, estimates of future additional and unreported losses, and other factors the Secretary may deem important (U.S. Treasury 2015). We show a simple example to work through the loss sharing mechanism.

Example 1. Consider a large insurer with \$100 billion in DEP the prior year. The insurer's TRIA deductible is equal to 20% of its DEP of \$100 billion, hence \$20 billion. Suppose that the aggregate loss due to terrorism events for the calendar year is \$40 billion, of which \$1 billion is paid by the policyholders from deductibles and coinsurances. For the insurance payment in excess of the \$20 billion TRIA deductible, 81% is shared by the government. Therefore, the government pays $\$(40 - 1 - 20) \times 0.81 = \15.4 billion, and the insurer is responsible for the remainder; i.e., $\$(40 - 1 - 15.4) = \23.6 billion. \square

1.3 Recoupment

In addition to the payment structure described above, the government is also mandated to follow a recoupment program for covered losses up to the industry retention level, set to \$37.5 billion for the year 2019⁶.

For all aggregate industry insured losses below \$37.5 billion, the federal government will recoup its payments at a 140% rate. The amount recouped is levied onto all insurers in the U.S. that offer TRIA-eligible commercial policies, and may be further levied onto their policyholders. For all losses above the market retention, the treasury has an option of recouping payments at its discretion. Since other alternatives exist for the government to fund these uncompensated outlays, it is hard to foresee what discretionary recoupment the government will employ. Therefore, it is often assumed in the literature that the Treasury only recoups the mandatory amount (Michel-Kerjan et al. 2018). In our proposal, we assume that the total recoupment amount is known and focus on the allotment of the recoupment to each insurer.

A visual representation of the recoupment scheme is shown in Figure 1.2.

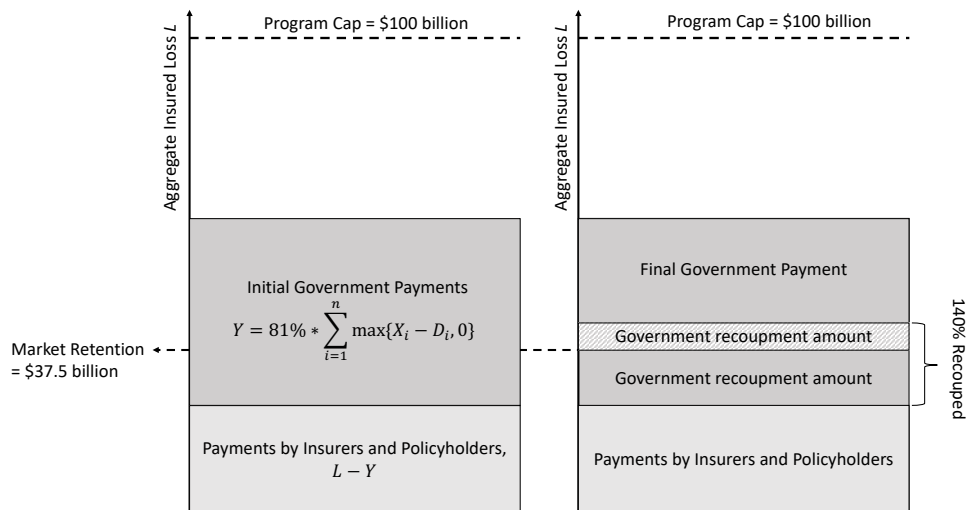


Figure 1.2: TRIA Recoupment Mechanism. Here, D_i is Insurer i 's TRIA deductible, equal to 20% of its prior year DEP, X_i is Insurer i 's insurance payout, and L is the aggregate insured loss. For outlays the federal government paid for insured losses below the market retention level, it recoups 140% of the outlays; for those paid for losses above the market retention level, it may recoup an amount at its discretion. The market retention level is set to \$37.5 billion for the year 2019; it was set to \$29.5 billion in 2015 and has been increasing by \$2 billion per year until 2019. The government share of 81% applies for the year 2019; it has been decreasing by 1% over the years since 2015 and is set to decrease by another 1% in 2020. See U.S. Treasury (2018) and Michel-Kerjan and Kunreuther (2018) for similar illustrations.

To illustrate this mechanism of the TRIA loss-sharing agreement, we add to Example 1.

Example 2. Recall that from Example 1, a \$40 billion insured loss would result in a payment of \$23.6 billion for the large insurer, \$1 billion for its policyholders, and \$15.4 billion for the

⁶TRIA's 2015 renewal states that the market retention be set to \$29.5 billion, increasing by \$2 billion until it hits \$37.5 billion in 2019.

government. Therefore, of the \$15.4 billion government payment, $\$(37.5 - 23.6 - 1) = \12.9 billion is under the market retention level. In this scenario, the government would recoup 140% of the payment under the retention level, hence $\$12.9 \times 1.4 = \18.1 billion. The remainder of $\$15.4 - \$12.9 = \$2.5$ billion is subject to discretionary recoupment.

In recap, a \$40 billion loss would fall as follows: The insurance company pays \$23.6 billion and its policyholders pay \$1 billion from policy deductibles and coinsurance. The government initially pays \$15.4 billion, but recoups \$18.1 billion plus a possible discretionary amount from the insurer, which can be further levied onto commercial policyholders. \square

When multiple insurers participate in the market, the U.S. Treasury would then be responsible for determining how the recoupment would be allotted among all insurers. As previously stated, there is no current method for how this amount should be recouped from each insurer. This paper proposes such a recoupment scheme.

1.4 Literature Review

Despite the importance of studying terrorism risk and terrorism insurance, there is limited research in this area in the literature. Some important and recent ones include Brown et al. (2004), Lakdawalla and Zanjani (2005), Michel-Kerjan and Pedell (2005), and Michel-Kerjan et al. (2015, 2018). These authors study terrorism insurance demand, investigate the economic impact of the government providing terrorism reinsurance, or compare and test the public-private partnerships in covering terrorism risk in several countries.

Specifically, Brown et al. (2004) find that the stock price effect of the TRIP is neutral at best – neutral for property-casualty insurance companies and mostly negative for the other industries affected by TRIA. Lakdawalla and Zanjani (2005) argue that the government subsidies for terrorism insurance is a discouragement to self-protection and in the meantime limit the negative externalities of self-protection (hurting national prestige, for instance). Michel-Kerjan and Pedell (2005) offer a comprehensive comparison of and point out some fundamental differences between the public-private terrorism risk sharing mechanisms in France, Germany, and the U.S. Michel-Kerjan et al. (2015) study corporate demand for terrorism insurance and conclude that it is price inelastic. Michel-Kerjan et al. (2018) test the sustainability of the public-private partnership in the U.S. by performing scenario analysis at different levels of terrorism losses.

Our paper is related to these studies but focuses on the recoupment process instead, which has been unclear and untested in practice so far, as also pointed out by Michel-Kerjan et al. (2018). We suggest a recoupment scheme that takes into account the spatial risk of terrorism attacks and is easy to implement.

1.5 Structure of the Paper

The rest of this paper consists of four sections. Section 2 introduces the theoretical frameworks for modeling the terrorism insurance policies, terrorism risk sharing, for modeling the geospatial terrorism risk, and proposes our recoupment scheme. Section 3 describes the data set we shall use to estimate our geospatial point process. Section 4 presents our analysis of the data, our estimation of the model, and an illustration of the recoupment scheme for a hypothetical insurance portfolio

based on the estimated terrorism risk. Finally, Section 5 concludes this paper.

Chapter 2

Model, Theory, and Proposal

2.1 Insurance Market

In this section, we introduce our model for the TRIA-eligible insurance market and for the risk sharing between the insurance companies, the government, and the policyholders.

Suppose that there are n insurers that participate in the market by offering TRIA-eligible insurance policies, which we denote by Insurers $1, \dots, n$. Also suppose that Insurer i has m_i policies in force, among which the j -th policy covers 100% of the policyholder's loss in the current year due to acts of terrorism in excess of the deductible d_{ij} , $i = 1, \dots, n$, $j = 1, \dots, m_i$. Let the current year's insured loss be L_{ij} for insurer i 's policy j . Thus, the aggregate insured losses from terrorism risks for insurer i and for the entire industry are given, respectively, by

$$L_i = \sum_{j=1}^{m_i} L_{ij} \quad \text{and} \quad L = \sum_{i=1}^n L_i = \sum_{i=1}^n \sum_{j=1}^{m_i} L_{ij}.$$

The insured loss of L_i will be shared between Insurer i , her policyholders, and the government. The policyholders are responsible for the losses below their policy deductibles d_{i1}, \dots, d_{im_i} , while the insurer and the government for the remainder. Let Insurer i 's payout be X_i and the government's reimbursement to Insurer i be Y_i . Assuming that the policies all have zero coinsurance, we have

$$X_i = \sum_{j=1}^{m_i} \max\{L_{ij} - d_{ij}, 0\}.$$

Suppose that insurer i 's TRIA deductible is D_i , meaning that the government reimburses the insurer for some amount of her losses only if the insurance payout to policyholders X_i is above D_i . Again, for 2019, the TRIA deductible D_i is 20% of the insurer's 2018 DEP, and the TRIA program is triggered only if the industry aggregate loss L exceeds \$180 million. When the aggregate loss L is over \$100 billion, the excess over \$100 billion is not covered by the government or the insurers. Although there is no set method for determining the pro rata loss percentage for losses over \$100 billion, a possible method is that the government reimburses each insurer an amount in proportion to her insured loss L_i . That is, the government's reimbursement to insurer i is given by

$$Y_i = 0.81 \max\{X_i - D_i, 0\} 1_{(180m \leq L \leq 100b)} + \left(100b - \sum_{i=1}^n D_i\right) \frac{L_i}{L} 1_{(L > 100b)},$$

where we use $1_{(\cdot)}$ to denote the indicator function and naturally assume that the insurers' TRIA deductibles have a sum below \$100 billion.

The government's total recoupment R contains two components: a mandatory recoupment equal to 140% of the government's outlays for losses over the industry retention level, which is \$37.5 billion in 2019, and a discretionary component for excess losses over the retention level. That is,

$$R = 1.4 \times \max \left\{ \min\{L, 37.5b\} - \sum_{i=1}^n (L_i - Y_i), 0 \right\} + \text{applicable discretionary recoupment}$$

In particular, if the aggregate loss L is not greater than \$37.5 billion, the government will recoup

140% of its outlays; that is $1.4 \sum_{i=1}^n Y_i$. We shall propose an allocation scheme for the government to allot the recoupment amount to each insurer.

2.2 A Geospatial Framework for Terrorism Risk

One may expect the chance of terrorist attacks to vary substantially by location; it is usually much higher for large cities than for rural areas. This motivates us to incorporate location information in our model. In this paper, we use a spatial point pattern to model the terrorism risk in the U.S.

Specifically, we consider terrorist attacks in the U.S. during the current year as points in a non-negative point process N that is defined on the two-dimensional space of the U.S., say, \mathcal{X} . The point process models the number of attacks for every region in the U.S. territory. For example, for a region B that is a compact set in \mathcal{X} , the non-negative variable $N(B)$ represents the random number of attacks that occur in B within the year.

Generally, the statistical properties of a point process can be characterized by its intensity function $\lambda(\mathbf{u})$, $\mathbf{u} \in \mathcal{X}$, which measures the expected number of points per unit area. We assume that the intensity function is a deterministic function, defined by

$$\lambda(\mathbf{u}) = \lim_{|\Delta\mathbf{u}| \downarrow 0} \frac{E[N(\mathbf{u}, \mathbf{u} + \Delta\mathbf{u})]}{|\Delta\mathbf{u}|}, \quad \mathbf{u} = (x, y) \in \mathcal{X},$$

where $|\Delta\mathbf{u}|$ is the area of $\Delta\mathbf{u}$, and $(\mathbf{u}, \mathbf{u} + \Delta\mathbf{u})$ represents the rectangle formed by \mathbf{u} and $\mathbf{u} + \Delta\mathbf{u}$. The intensity measure of the point process, defined by

$$\mu(B) = \int_B \lambda(\mathbf{u}) d\mathbf{u}, \quad \mathbf{u} \in \mathcal{X}$$

for $B \subseteq \mathcal{X}$, measures the expected number of attacks that occur in region B ; that is,

$$\mu(B) = E[N(B)], \quad B \subseteq \mathcal{X}.$$

For Insurer i that provides coverages at locations $\mathbf{u}_1, \dots, \mathbf{u}_{m_i}$, we use

$$\Lambda_i = \sum_{j=1}^{m_i} \lambda(\mathbf{u}_j) \tag{2.1}$$

to measure her (frequency) risk of terrorism. Note that $\Lambda_i |\Delta\mathbf{u}|$ is the expected number of attacks around the $\Delta\mathbf{u}$ neighborhoods of these locations; Λ_i itself is not exactly the expected number of attacks at the locations. Nonetheless, the value of Λ_i offers a good indication of relative (frequency) risk of terrorism, and it will serve our purpose of designing a recoupment scheme.

We would like to point out that private firms such as Risk Management Solutions (RMS) and Applied Insurance Research (AIR) have also developed commercial packages to evaluate terrorism risks. While we model the number of terrorist attacks, RMS bases their terrorism risk model on a probabilistic method, measuring the relative likelihood of attacks given different cities, targets, and attack modes (Willis et al. 2007). The number of attacks obviously matters in loss modeling.

AIR also offers a similar probabilistic model, as well as a geospatial model. So far we do not have access to detailed descriptions of AIR’s models.

2.3 Proposed Recoupment Scheme

We first use a simple example to show why some straightforward recoupment schemes may not work satisfactorily. To illustrate, consider two insurance companies, labeled as Insurers 1 and 2, which provide terrorism risk coverage in Cities A and B, with DEPs listed in Table 2.1 below:

Table 2.1: A simple example to illustrate recoupment ideas

Insurer	DEP last year	DEP this year (before recoupment)	DEP this year (after recoupment)	Current coverage
1	P_1	\tilde{P}_1^{br}	$\tilde{P}_1^{ar} = \tilde{P}_1^{br} + R_1$	City A
2	P_2	\tilde{P}_2^{br}	$\tilde{P}_2^{ar} = \tilde{P}_2^{br} + R_2$	City B

Now suppose that terrorist attacks occurred last year in City A at several locations covered by Insurer 1. The insured loss incurred was large enough to trigger the TRIA program but was below the market retention level, so that the government will pay a reimbursement, Y_1 , to Insurer 1 and will later recoup the mandatory amount of $1.4Y_1$. The total recoupment R is allocated to the two insurers, with R_1 to Insurer 1 and R_2 to Insurer 2.

A straightforward recoupment idea is to recoup amounts proportional to the insurers’ DEPs collected last year; i.e., to recoup

$$R_1 = \frac{P_1}{P_1 + P_2}R \quad \text{and} \quad R_2 = \frac{P_2}{P_1 + P_2}R, \quad (2.2)$$

in the hope that the DEPs offer a good indication of the insurers’ terrorism risk. Nonetheless, it is important to notice that the DEPs P_1 and P_2 are last year’s premiums and are calculated using historical data of attacks prior to last year. For estimations of terrorism risk, where occurrences are generally rare, a handful of new occurrences may overhaul the perception of the risk of a certain region altogether. It may indicate that City A has just become a target of the terrorists and may reveal vulnerabilities of this region, leading to higher chances of future attacks. It is important that we update our assessment of terrorism risk with this information accounted for, and important that the recoupments reflect the actual risk the government has covered for the insurers, not the risk estimated based only on “outdated” data.

Motivated by the analysis above, one may consider recouping based on the (before-recoupment) premiums the insurers are to collect this year, thinking that the updated premiums will reflect the

updated terrorism risk; i.e., consider recouping

$$R_1 = \frac{\tilde{P}_1^{br}}{\tilde{P}_1^{br} + \tilde{P}_2^{br}} R \quad \text{and} \quad R_2 = \frac{\tilde{P}_2^{br}}{\tilde{P}_1^{br} + \tilde{P}_2^{br}} R. \quad (2.3)$$

However, there are challenges and limitations for the government to implement such a scheme. One is that, to implement this recoupment scheme, the government needs to know upfront, at the time of recoupment, the (before-recoupment) premiums to be collected for this current year for all the insurers. But collecting such information so that it is immediately available to the government is a big challenge. The government could issue data calls, but there is no guarantee that the data collections can be completed for the government to announce the recoupment amounts in a timely manner. Moreover, imagine an unlikely situation that one insurer, say, Insurer 2, quits insuring commercial properties and collects zero DEP for this year. Recouping zero from Insurer 2 just because she quits and collects zero DEP now, as suggested under recoupment scheme (2.3), is not wise; after all, Insurers 2 did receive reimbursement for the insurance she used last year.

We propose to recoup

$$R_1 = \frac{\tilde{\Lambda}_1 P_1 / \Lambda_1}{\tilde{\Lambda}_1 P_1 / \Lambda_1 + \tilde{\Lambda}_2 P_1 / \Lambda_2} R \quad \text{and} \quad R_2 = \frac{\tilde{\Lambda}_2 P_2 / \Lambda_2}{\tilde{\Lambda}_1 P_1 / \Lambda_1 + \tilde{\Lambda}_2 P_1 / \Lambda_2} R, \quad (2.4)$$

where Λ_i and $\tilde{\Lambda}_i$ are measurements of frequency risk defined in (2.1) and in practice are estimated, respectively, using data prior to last year and data with last year included. In general, when there are n insurers, each insurer is recouped an amount of

$$R_k = \frac{1}{\sum_{i=1}^n \frac{\tilde{\Lambda}_i P_i}{\Lambda_i}} \frac{\tilde{\Lambda}_k P_k}{\Lambda_k} R, \quad k = 1, \dots, n. \quad (2.5)$$

Our idea of using such a recoupment scheme is that the recoupment can be understood as an insurance premium paid for using the insurance during the past year; i.e., a retrospective insurance premium. It should reflect the actual frequency and severity risks covered by the federal government during the past year. While the severity risk is generally stable over time, largely depending on the value of the property covered, number of employees working in the covered property, etc., the frequency risk gets a substantial update when recoupment is needed (meaning that major attacks have occurred). It is reasonable to assume that the private insurers, through their underwriting processes, have gained better information than the government about potential property damages, potential workers compensation payments, etc., when the properties under coverage are attacked, and hence know their severity risk better. On the other hand, because of the Treasury's certification process required for TRIA-eligible insurance payments, the government should be equally well, if not better, informed about the frequency risk of terrorist attacks. Therefore, when developing a recoupment scheme, it is natural for the government to take advantage of the severity risk information from the private insurers while supplying their own assessment of frequency risk.

In our recoupment scheme, we use the updated frequency risk estimated based on last year's attacks, reflected by $\tilde{\Lambda}_k$, $k = 1, \dots, n$. As we shall demonstrate later, these are quantities the government can estimate using data available. In the meantime, we also try to incorporate the severity risk the government covers for each insurer. The premiums charged by the insurers reflect

the severity risk level; in fact, the severity risk can be measured roughly by P_i/Λ_i for Insurer i . Again, this is based on last year's figures that are supposedly already known to the government, either through regulation report filings or through past data calls. Hereafter, we focus on how to update the frequency risk for implementing the proposed recoupment scheme through estimating a geospatial model.

Chapter 3

Data

3.1 Global Terrorism Database

We use data from the Global Terrorism Database (GTD) to illustrate our methodology. The GTD is a project run by The National Consortium for the Study of Terrorism and Responses to Terrorism, at the University of Maryland. It is an open-source database that collects information on terrorist events around the globe dating back to 1970. The data is updated on a bi-yearly basis and now includes over 180,000 incidents of terrorism. The GTD was developed to be a comprehensive set of data on domestic and international terrorism, allowing researchers to better understand the nature of this risk.

Note that some events in the database may not be certified by the Treasury as acts of terrorism. One main difference between the definition of terrorism acts within the GTD¹ and the Treasury, is that the latter has a \$5 million threshold for certification. An exemplar event that has not been certified by the Treasury is the 2013 Boston Marathon bombing. Risk managers have urged better risk certification after the Boston bombing². For our analysis of attack frequency, the severity threshold of \$5 million should not play a role, and hence we use the events listed in the GTD when estimating the intensity.

The GTD contains 75 coded variables we can utilize for data analysis, and there are up to 120 total attributes for each attack. For the scope of our paper, we focus on latitude and longitude variables to assess geospatial risk. We also utilize a success variable, coded as 1 if the terrorist attack succeeds and 0 otherwise³. For part of our initial exploratory data analysis, we also use a variable that encodes known property damages sustained during an attack. We adjusted these figures for inflation at 2017 dollars⁴.

We limit our data analysis to events perpetrated inside the continental U.S. An illustration of these attacks during 1970–2016 is shown in Figure 3.1, where successful attacks are shown in red.

¹See page 10 of Data dictionary, available at <https://www.start.umd.edu/gtd/downloads/Codebook.pdf>

² See, e.g., www.insurancejournal.com/news/national/2015/03/18/360930.htm.

³Note that for our analysis, we only consider attacks that are deemed successful.

⁴Inflation figures used are from the CPI of the U.S. Bureau of Labor Statistics.

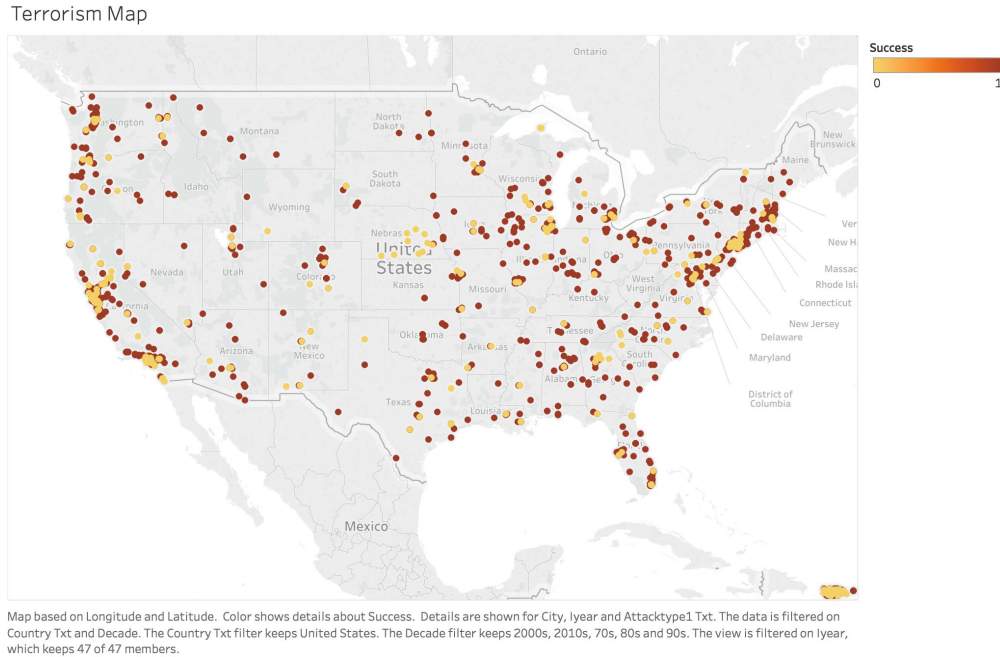


Figure 3.1: Map of Terrorist Attacks 1970-2016. This graph is generated using the data up to 2016 (inclusive) from the Global Terrorism Database. We plot the latitudes and longitudes of the attacks that occurred in continental United States, where red dots represent successful attacks and yellow dots represent failed attempts.

We also list the total number of attacks by states in Appendix 5.1. To assess the geospatial risk, we must determine if the spatial points in Figure 3.1 look homogeneous across the U.S. The first thing we can observe from the figure, is the clustering of attacks near large metropolitan areas. There are clear clusters in cities such as New York, San Francisco, Los Angeles, and Chicago. Therefore, our first impression is that occurrences are not spatially homogeneous. We shall test this hypothesis of homogeneity and present our findings in Section 4.

Chapter 4

Empirical Studies

4.1 Data Analysis and Model Estimation

In order to see whether the attack occurrences are independent or exhibit clustering, we perform exploratory analysis for determining spatial correlation in point patterns. Traditionally, some popular techniques used to determine spatial correlation are Ripley's K-function and the pair correlation function (PCF); see Baddeley et al. (2015) for detailed discussions on the K-function and PCF. Note that both functions are defined under an assumption of homogeneity for the underlying point process, which we anticipate not to be the case upon visual inspection of Figure 3.1. Hence, we opt for the inhomogeneous K-function and the inhomogeneous PCF when testing for clustering in our data. Note that both tests apply border corrections to our data. Since many of the points in our spatial data are near borders of the U.S. map, it is important to add adjustments to make sure contributions from edge locations (such as New York, San Francisco, and Los Angeles) are properly accounted for.

4.2 Inhomogeneous K-function

The K-function is an often-used technique for analyzing spatial correlation through the assumption of homogeneity. Since we suspect our data is not homogeneous, we use the inhomogeneous K-function instead since this corrects for the in-homogeneity of the spatial intensity, along with the window area.

Suppose that N is a point process with intensity $\lambda(u)$ at point u , and u is a location within N . With the addition of corrections to the window area and intensity inhomogeneity, the theoretical inhomogeneous K-function is then defined as

$$K_{inhom}(r) = E[\text{number of } r\text{-neighbors of } u \mid N \text{ has a point at location } u].$$

In words, assuming there is a random point belonging N at a location u , the inhomogeneous K-function is equal to the expected number of other points of N within a radius distance r of location u , corrected by the process intensity and window area (Baddeley, Rubak and Turner 2015).

This theoretical function can be estimated using the empirical inhomogeneous K-function $\hat{K}_{inhom}(r)$ for point patterns. $\hat{K}_{inhom}(r)$ is the cumulative average number of points lying within a radius r of a data point. This is typically corrected for edge effects, and standardized as previously discussed. The correction and standardization allows for comparison between different spatial patterns in different observation windows.

Let two points, x_i and x_j , have distance d_{ij} between them. Also let \mathcal{X} be a spatial window in the shape of the U.S. with area $|W|$, and let the edge correction be $e_{ij}(r)$. Now, let all points x_i have weight equal to the inverse of the intensity at point i defined by $w_i = 1/\lambda(x_i)$. Similarly all pairs of points will be weighted by the inverse of the product of each intensity function. That is to say weight $w_{ij} = 1/[\lambda(x_i)\lambda(x_j)]$.

We can estimate the inhomogeneous K-function as

$$\hat{K}_{inhom}(r) = \frac{1}{D^p |W|} \sum_{i=1}^n \sum_{j=1, j \neq i}^n \frac{1}{\lambda(x_i)\lambda(x_j)} 1_{(d_{ij} \leq r)} e_{x_i, x_j}(r),$$

where D^p refers to the p th power of D such that

$$D = \frac{1}{|W|} \sum_i \frac{1}{\hat{\lambda}(x_i)}.$$

We can use this empirical estimate to analyze our data and look for signs of clustering. Graphs of $\hat{K}_{inhom}(r)$ that plot above the theoretical Poisson process line are consistent with clustered data. Plotting near the Poisson line is consistent with independence and spatial randomness. Note that the theoretical Poisson line is given by $K_{pois} = \pi r^2$ since that is the number of points we expect inside a circle of radius r given that it is corrected for its intensity $\lambda(u)$.

Additionally, we can plot process envelopes around our theoretical K_{pois} to assess if our estimated function shows significant signs of clustering. Lines that fall outside of the envelopes are considered statistically significant with a p-value of $1/(s+1)$, where s is the number of simulations given to calculate the envelope¹. Note that envelopes can be global or pointwise. Global envelopes create a band of maximum deviations for the entire process, while pointwise envelopes create a 95% band at each radius.

Our spatial data results in the following graphs shown in Figure 4.1.

¹Here, we set s to 19 for a resulting significance level of 5%.

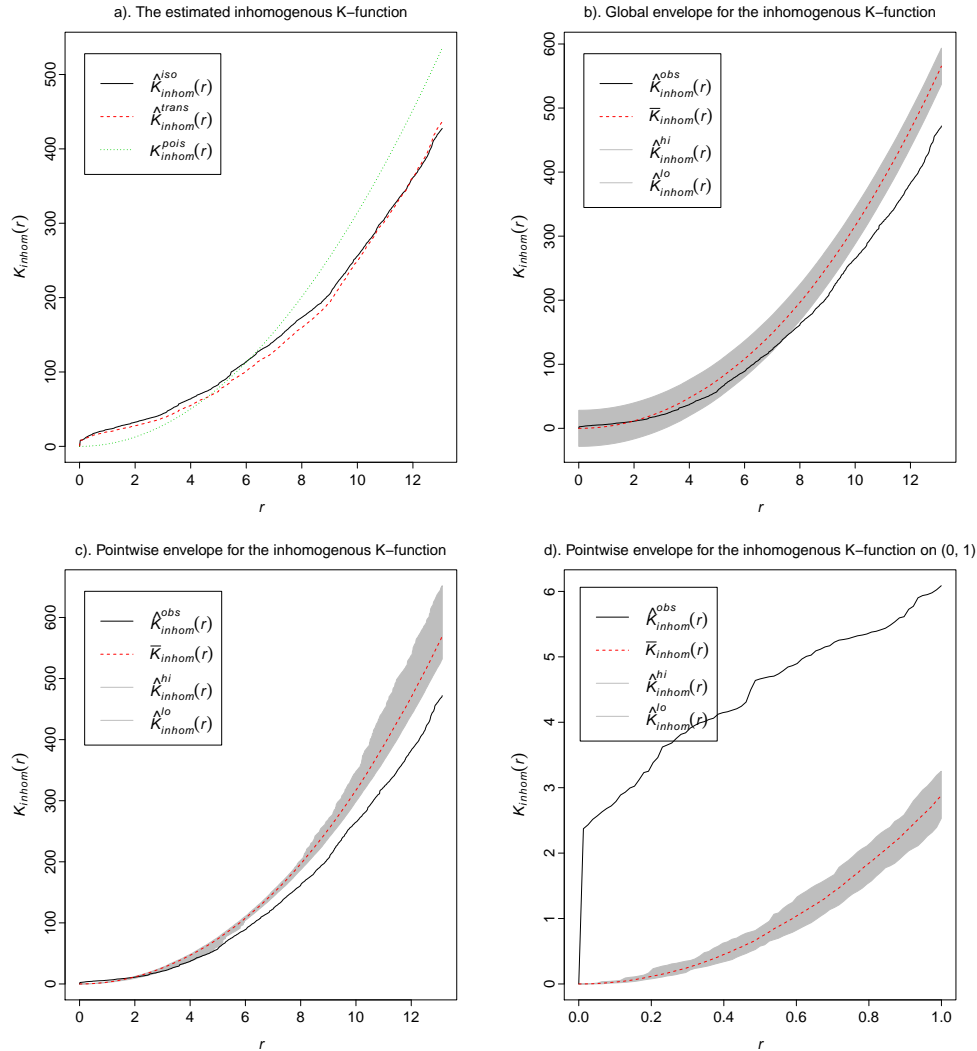


Figure 4.1: Inhomogeneous K-function Analysis. This figure shows our exploratory analysis of the spatial data using the inhomogeneous K-function. Graph a) shows the estimated inhomogeneous K-function. Note that for small radii, the estimated functions (shown in black and red) plot above the theoretical homogeneous process line (shown in green), indicating existence of clusters in the data. Graph b) shows the global envelope for the inhomogeneous K-function. Graphs c) and d) show pointwise envelopes, where d) is a zoomed-in version of c) with domain restricted to $r \leq 1$.

In plot a), we can see the theoretical K_{pois} in green, with our estimated inhomogeneous K-functions plotted in black and red, showing isotropic and translational edge corrections respectively. Note that at small radii ($r \leq 4$), the estimated inhomogeneous K plots above the Poisson line, which is consistent with clustered data. In words, we see a higher proportion of points at small distances from one another than we would expect.

Plot c) of Figure 4.1 shows the global envelope for this process, while plots c) and d) show the pointwise envelope, with d) restricting the domain to $r \leq 1$. Note that the global envelope takes into account the maximum deviations for the function on its entire domain, therefore producing a maximum and minimum value that would suggest our clustered data is not significant. However, we focus on smaller radii since clusters of points are ones close to each other. We can see from the

pointwise envelope that our estimated inhomogeneous K-function falls well above the 95% band, thus leading to a conclusion that our spatial data is clustered at a 95% confidence level.

4.3 Inhomogeneous Pair Correlation Function

Another useful tool we can implement in our data analysis is the inhomogeneous PCF $g_{inhom}(r)$. In contrast to the inhomogeneous K-function, the inhomogeneous PCF gives the contributions of distances *equal* to r , rather than *less* than r . That is to say we count the number of points inside a ring with a given width, rather than a circle with a given radius. Note that the regular PCF assumes homogeneity, leading us to use its inhomogeneous counterpart.

Let $K'_{inhom}(r)$ be the derivative of the inhomogeneous K-function with respect to r . The inhomogeneous PCF is defined on two-dimensions as

$$g_{inhom}(r) = \frac{K'_{inhom}(r)}{2\pi r}.$$

Note that $2\pi r$ is the derivative of the theoretical K-function for a homogeneous Poisson process. Therefore, the inhomogeneous PCF can also be described as the probability of observing an inter-point distance of r divided by that probability for a homogeneous Poisson process.

If $g_{inhom}(r) = 1$, the conclusion is that the spatial data is independent. Values of $g_{inhom}(r)$ greater than 1 for radius r point to clustering of the data, since there are many more observations with inter-point distance r than expected.

We can estimate the inhomogeneous PCF by implementing kernel smoothing with kernel κ . For example, common kernels used are Epanechnikov or Gaussian. Bandwidths are selected by default using Stoyan's Rule of Thumb². We can also use the derivative of $\hat{K}_{inhom}(r)$ previously shown in graph a) of Figure ??.

The graph of a clustered spatial pattern should spike at small radii, before converging to 1 at larger radii. This is due to the fact that many points are clustered and contribute to a ring of smaller radius. Similar to the inhomogeneous K-function, we can also plot global and pointwise envelopes to assess significance. Our results are shown in Figure 4.2.

²See <https://rdr.io/github/spatstat/spatstat/man/bw.stoyan.html> for further discussion.

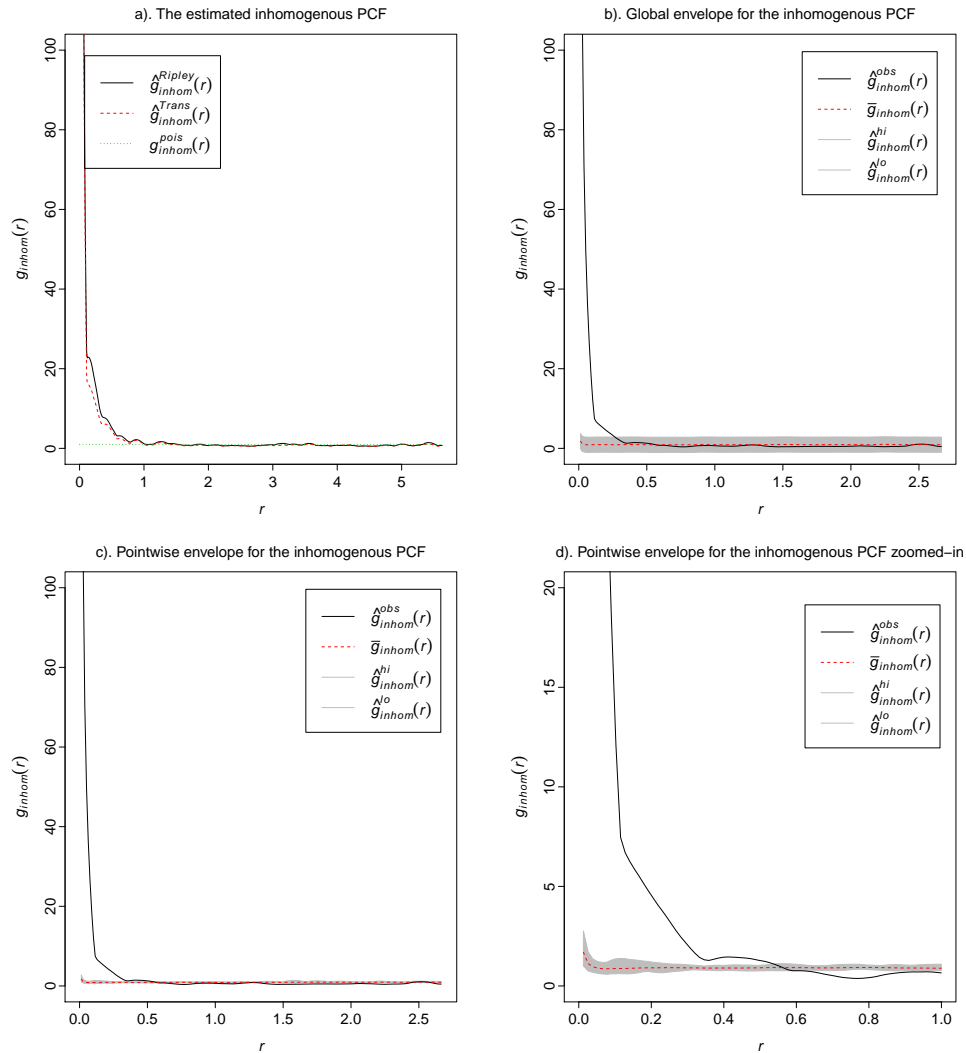


Figure 4.2: Inhomogeneous PCF Analysis. This figure shows our exploratory analysis of the spatial data using the inhomogeneous PCF. The gray areas represent the 95% confidence bands. Graph a) shows the estimated inhomogeneous PCF. Note that for small radii, the estimated functions (shown in black and red) spike above the theoretical homogeneous process line (shown in green), indicating existence of clusters in the data. Graph b) shows the global envelope for the inhomogeneous PCF. Graphs c) and d) show pointwise envelopes, where d) is a zoomed-in version of c) with domain restricted to $r \leq 1$.

As previously noted, clustered spatial patterns exhibit a spike at smaller radii before converging to 1 as the radius increases. Our data, shown in panel a) is consistent with this description. From the global and pointwise envelopes in plots b) through d), we can see that our clustered data is significant at a 95% confidence level, as the estimated inhomogeneous PCF falls outside both the global deviations and the pointwise deviations at small radii. This again leads to a conclusion of statistically significant clustering within our data.

4.4 Our Model

From the tests for spatial correlation, we can conclude that our data is not homogeneous, and is in fact clustered. We opt for a non-parametric model due to its flexibility in recognizing clusters of spatial points. Given a spatial window with the shape of the U.S., we can utilize Gaussian kernel smoothing with edge corrections and a bandwidth of 1 to calculate the intensity of terrorism attacks at given latitudes and longitudes. Note that larger bandwidths may result in risk spreading too wide from attack clusters, and could diminish the effects of updated frequencies after an attack.

We divide the given intensities by the number of years of data we have available, creating an annualized intensity estimate of attacks across the U.S. from 1970-2016³.

The results are shown in Figure 4.3.

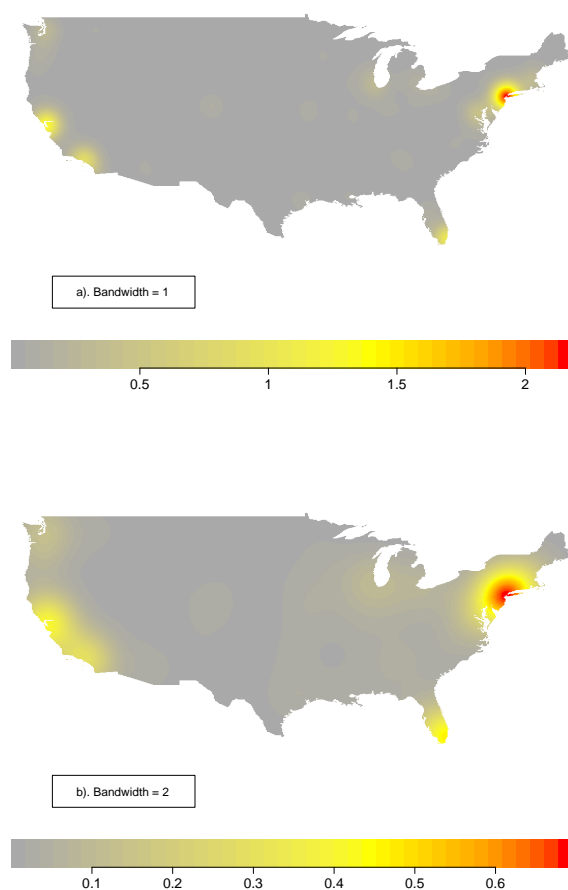


Figure 4.3: Estimated Intensities. This figure shows an estimated annual intensity using the data up to 2016 (inclusive) from the Global Terrorism Database. We use non-parametric Gaussian kernel smoothing to estimate the intensity. The top image shows the intensity estimated using a bandwidth of 1, while the bottom image shows the intensity estimated with a bandwidth of 2.

³Note that smoothing is dependent on the number of image pixels, and we use a 1024x1024 pixel resolution map of the U.S.

Note that graph a) of Figure 4.3 shows the intensity with a bandwidth of 1, while b) shows a bandwidth of 2. The intensity estimation is consistent with our initial assumptions of clustered patterns located at large cities. We list some notable cities used in later examples, and their annualized intensity λ_{annual} in Table 4.3.

Table 4.3: Annualized intensities for notable cities

City	λ_{annual}
New York	2.183
Los Angeles	0.869
San Francisco	1.310
Chicago	0.293
Las Vegas	0.020

4.5 Suggested Recoupment for a Hypothetical Portfolio

As previously proposed, our recoupment scheme for a marketplace with n insurers follows

$$R_k = \frac{1}{\sum_{i=1}^n \frac{\tilde{\Lambda}_i P_i}{\Lambda_i}} \frac{\tilde{\Lambda}_k P_k}{\Lambda_k} R, \quad k = 1, \dots, n,$$

where R_k is the recouped amount from insurer k , and R is the total government recoupment. We use this proposed recoupment formula to follow through a hypothetical portfolio.

Suppose our portfolio consists of five insurers: Insurer 1, Insurer 2, ... Insurer 5. Also suppose that our portfolio only consists of five cities: New York, Los Angeles, San Francisco, Chicago, and Las Vegas. Let Insurer 1 only cover New York risk, Insurer 2 only cover Los Angeles risk, etc. In order to apply our recoupment mechanism, we must find the intensity of risk at each location, and we must find a way to estimate the DEP at each city.

While the latter is not available to the public, the U.S. Census Bureau publishes the total number of firms registered per city⁴. Here, we make the assumption that direct earned premiums are proportional to the number of firms in a given city⁵.

To calculate the annualized intensity at each city from one year to the next, we use a density function calculated from our model. In our hypothetical example, we compare the years 2015 and 2016. For example, upon computing the intensity of terrorist attacks at each location in 2015, we divide this number by 46 since there are 46 years from 1970 to 2015. We perform the same calculation in 2016 with 47 years of data.

⁴City information can be found in <https://www.census.gov/quickfacts/fact/table/US/PST045217>.

⁵Firms are defined as any individual proprietorships, partnerships, or any type of corporation filing with the Internal Revenue Service, with receipts exceeding \$1,000.

Table 4.4: A simple example to illustrate hypothetical recoupments

Insurer (City)	Original intensity	Updated intensity	Ratio $\tilde{\Lambda}_k/\Lambda_k$	Number of registered firms
Insurer 1 (New York)	2.187	2.183	0.998	1,050,911
Insurer 2 (Los Angeles)	0.882	0.869	0.985	497,999
Insurer 3 (San Francisco)	1.337	1.310	0.980	116,803
Insurer 4 (Chicago)	0.300	0.293	0.980	291,007
Insurer 5 (Las Vegas)	0.010	0.020	2.003	55,856

In Table 4.4, we let 2015 risk be the previous year's risk given by Λ_k , while 2016 represents the updated risk $\tilde{\Lambda}_k$. Note that the ratio for Insurer 5 (who only covers risk in Las Vegas), is significantly higher than the remaining insurers, which is a reflection of increasing terrorism risk. Up to 2015, Las Vegas had only ever experienced two successful terrorist attacks. In 2016 alone, they faced three separate events.

To continue our hypothetical example, we assume that premium is proportional to registered firms in a city. For simplicity, assuming a total DEP in all five cities to be \$100 billion, the DEP would be split as follows.

Table 4.5: A simple example to illustrate hypothetical recoupments, continued

Insurer (City)	Number of registered firms	DEP (in billions)	$\tilde{\Lambda}_k/\Lambda_k$ (2016/2015)
Insurer 1 (New York)	1,050,911	52.2	0.998
Insurer 2 (Los Angeles)	497,999	24.7	0.985
Insurer 3 (San Francisco)	116,803	14.5	0.980
Insurer 4 (Chicago)	291,007	5.8	0.980
Insurer 5 (Las Vegas)	55,856	2.8	2.003

In Table 4.5, note that the DEP column represents our premium, P_k , collected in 2015. We conclude our hypothetical example by calculating R_k for each insurer k , using Formula 2.5. Additionally, we calculate R_k as a percent of the DEP, assuming the government needs to recoup $R = \$8$ billion.

Table 4.6: A simple example to illustrate hypothetical recoupments, continued

Insurer (City)	P_k	$\tilde{\Lambda}_k/\Lambda_k$	R_k	R_k as % of premium
Insurer 1 (New York)	52.2	0.998	51.15%	7.84%
Insurer 2 (Los Angeles)	24.7	0.985	23.92%	7.73%
Insurer 3 (San Francisco)	14.5	0.980	5.58%	7.69%
Insurer 4 (Chicago)	5.8	0.980	13.90%	7.69%
Insurer 5 (Las Vegas)	2.8	2.003	5.46%	15.73%

Upon first look from Table 4.6, we can see that most of the recoupment falls on Insurer 1, who covers only New York risk. This makes intuitive sense since most of the premium, and therefore the severity risk, is in New York.

However, as we see from Column 5 of Table 4.6, policyholders for Insurer 5 in Las Vegas will be surcharged the most. While most of the recoupment falls on large cities with substantial earned premiums, the reflection of steady terrorism risk means policyholders from Insurers 1 through 4 would be surcharged at a comparable rate, slightly under 8%. Due to the increasing terrorism risk in Las Vegas, we can see that policyholders for Insurer 5 would be surcharged 15.73% of their premiums. Again, this is a reflection of the fact that Las Vegas has experienced five successful terrorist attacks since 1970, with three of them occurring in 2016.

Chapter 5

Concluding Remarks

5.1 Conclusion

In this paper, we propose a recoupment scheme for the Treasury to allot the required recoupment to the insurers that offer TRIA-eligible coverage. Our recoupment scheme takes into account both the frequency risk and severity risk of terrorism attacks. We use the intensity of a geospatial point process that counts the number of attacks in the U.S. to model the frequency risk and infer about the severity risk from the insurer's DEP. Both the frequency and severity risks are available to the Treasury, either through estimations of the point process or through insurers reports last year. Moreover, we suggest that, when recoupment is needed, indicating attacks have occurred, it will be important to update the intensity to reflect the true frequency risk that the government has covered, although the severity risk, which largely depends on, for example, the values of the properties covered, can still be reasonably approximated using corresponding quantities from last year. Using the Global Terrorism Database, we estimate a non-parametric model for the geospatial point process, and demonstrate that our proposed recoupment scheme is easily implementable. We hope that solving this challenge and providing a clear guideline to recoupment could contribute to the sustainability of the program.

Appendices

Appendix A: Attacks by State

Table 1: Number of Attacks by State, 1970-2016

State	Number of attacks
Alabama	16
Alaska	1
Arizona	34
Arkansas	5
California	595
Colorado	45
Connecticut	17
Delaware	3
DC	83
Florida	158
Georgia	29
Hawaii	4
Idaho	14
Illinois	112
Indiana	22
Iowa	24
Kansas	14
Kentucky	4
Louisiana	22
Maine	4
Maryland	35
Massachusetts	57
Michigan	45
Minnesota	25
Mississippi	11
Missouri	39
Montana	6
Nebraska	24
Nevada	18
New Hampshire	10
New Jersey	47
New Mexico	24
New York	515
North Carolina	34
North Dakota	6
Ohio	51
Oklahoma	15
Oregon	67
Pennsylvania	33
Rhode Island	2
South Carolina	5
South Dakota	9
Tennessee	24
Texas	63
Utah	20
Vermont	5
Virginia	42
Washington	101
West Virginia	2
Wisconsin	37
Wyoming	2

Appendix B: Log-Gaussian Cox Process

In Section 4.4, we discussed a Gaussian Kernel-Smoothing approach to calculating the intensity of terrorist attacks across the United States. While this offers flexibility in recognizing clusters within spatial patterns, we could also consider fitting a parametric model to our data. One such way to accomplish this is by fitting a Log-Gaussian Cox Process (LGCP) model. This is an important future step in our research regarding estimation of terrorism risk. The details of LGCP's are discussed below.

Recall that a Poisson Process is a counting process for event occurrences based on a deterministic intensity function $\lambda(\mathbf{u})$. A Cox Process, sometimes referred to as a doubly stochastic point process, replaces such intensity function with a random field. More specifically, this random field is denoted as the random driving intensity $\Lambda(\mathbf{u})$, where intensities are realizations of the random field. Moreover, we state the intensity $\lambda(\mathbf{u}) = E[\Lambda(\mathbf{u})]$.

In the case of a Log-Gaussian Cox Process, we model the log intensities $\ln\lambda(\mathbf{u})$ to assure positive values for the intensity. Additionally, the driving intensity is modeled as a gaussian random field.

Let $\ln\lambda(\mathbf{u})$ be the log intensity (i.e. log of the expected driving intensity) of terrorist attacks at a function of space \mathbf{u} . In order to understand the behavior of the gaussian random field, we model a Log-Gaussian Cox Process in the form:

$$\ln\lambda(\mathbf{u}) = B(\mathbf{u}) + \theta^T * \mathbf{Z}(\mathbf{u}), \quad (1)$$

where $B(\mathbf{u})$ represents an intercept, and $\theta^T * \mathbf{Z}(\mathbf{u})$ is the set of coefficients and variables in the model.

Much like linear regression in how we attempt to predict a continuous outcome based on certain variables, we can utilize location-dependent variables to predict attack intensity. For example, we can use population and economic indices at different locations in the United States to predict the density of terrorist attacks.

Our first thought about the choice of the covariate function $\mathbf{Z}(\mathbf{u})$ is the population and/or economic index at the location (u), since we may reasonably expect terrorism attacks are more likely to occur at more populated and economically developed areas. Data for population and economic indices are available at the metropolitan-area level¹. Metropolitan areas provide a large enough area to differentiate population and GDP values, but small enough to provide a granular look at terrorist intensity. Since terrorist attacks may occur in non-metropolitan areas, a model could utilize population and GDP values dependent on if attacks are located in metropolitan areas, assigning a constant intercept for intensity in non-metropolitan areas. Fitting a full model based on these variables and the form introduced in Appendix B Equation 1, we could predict terrorism intensity as such, where 1_* is the indicator function:

$$\ln\lambda(\mathbf{u}) = \beta_0 + \beta_1 * Population(u) * 1_{Metro} + \beta_2 * GDP(u) * 1_{Metro} + \beta_3 * 1_{NotMetro} \quad (2)$$

This would allow us to answer the question – How much of the spatial variation of terrorist attacks can we explain through variations in population and GDP.

¹Data can be found at the Bureau of Economic Analysis at <https://www.bea.gov/>.

Bibliography

- [1] Baddeley, A.; Rubak, E.; Turner, R. *Spatial Point Patterns: Methodology and Applications with R*. Chapman and Hall/CRC, 2015.
- [2] Brown, J. R.; Cummins, J. D.; Lewis, C. M.; Wei, R. An empirical analysis of the economic impact of federal terrorism reinsurance. *Journal of Monetary Economics* 51 (2004), 861–898.
- [3] Chesney, M.; Reshetar, G.; Karaman, M. The impact of terrorism on financial markets: An empirical study. *Journal of Banking & Finance* 35 (2011), 253–267.
- [4] Willis, H.; LaTourrette, T.; Kelly, T.; Hickey, S.; Neill, S. *Terrorism risk modeling for intelligence analysis and infrastructure protection*, 2007.
- [5] Lakdawalla, D.; Zanjani, G. Insurance, self-protection, and the economics of terrorism. *Journal of Public Economics* 89 (2005), 1891–1905.
- [6] Michel-Kerjan, E.; Pedell, B. Terrorism risk coverage in the post-9/11 era: A comparison of new public–private partnerships in France, Germany and the US. *The Geneva Papers on Risk and Insurance-Issues and Practice* 30 (2005), 144–170.
- [7] Michel-Kerjan, E.; Kunreuther, H. A successful (yet somewhat untested) case of disaster financing: Terrorism insurance under TRIA, 2002–2020. *Risk Management and Insurance Review* 21 (2018), 157–180.
- [8] Michel-Kerjan, E.; Raschky, P.; Kunreuther, H. Corporate demand for insurance: new evidence from the US terrorism and property markets. *Journal of Risk and Insurance* 82 (2015), 505–530.
- [9] National Consortium for the Study of Terrorism and Responses to Terrorism (START). (2018). *Global Terrorism Database [Data File]* Retrieved from <https://www.start.umd.edu/gtd>
- [10] U.S. Treasury. *Terrorism risk insurance program re-authorization act of 2015*, 2015.
- [11] U.S. Treasury. *The Process for Certifying an “Act of Terrorism” under the Terrorism Risk Insurance Act of 2002*, October 2015
- [12] U.S. Treasury. *Report on the overall effectiveness of the Terrorism Risk Insurance Program*. Washington, DC, June 2018.

Academic Vita

EDUCATION:

The Pennsylvania State University, Schreyer Honors College, University Park, PA
Bachelor of Science Degree in Mathematics – Actuarial Option
Minor in Statistics

Class of 2019

ACTUARIAL EXAMS:

- **Exams 1/P, 2/FM, 3/IFM, MAS-I:** Passed *Oct 2018*
- **Exam MAS-II:** Sitting *Apr 2019*
- **Economics, Corporate Finance, Applied Statistical Methods VEE:** Credit Earned *May 2018*

JOB EXPERIENCE:

CNA Insurance, Chicago, IL *May - Aug 2018*
Summer Actuarial Intern – Specialty Lines Department

- Constructed a holistic view of the cyber-security insurance book, and streamlined the process for monthly reviews
- Created an early-warning algorithm to detect significant shifts in the specialty lines book of business

Erie Insurance, Erie, PA *May - Aug 2017*
Summer Actuarial Intern – Personal Pricing Department

- Improved base rate development for private passenger auto after completing study on metropolitan area rate suppression
- Reverse-engineered 4 Conning market indices and reprogrammed DFA simulations, resulting in \$10,000 annual savings
- Programmed Watson IBM to answer 100 common questions from agents/policyholders in Underwriting case competition

MyStem Academy, Pittsburgh, PA *Jun 2010 – Aug 2016*
Robotics Instructor

- Taught multi-level programming courses to over 700 children, culminating in completion of sponsored LEGO challenges
- Trained over 20 instructors to teach similar robotics courses, building a base for future STEM education in Pittsburgh

University of Pittsburgh Cancer Institute, Pittsburgh, PA *Jun - Aug 2014*
Computational Biology Department

- Utilized Python to extract molecular data from web databases and track most commonly found compound shapes
- Traced over 1 million molecular paths which are used today by UPCI labs in drug-targeting tests

National Robotics and Engineering Center, Pittsburgh, PA *Jun - Aug 2013*
CMU Robotics Academy

- Instructed over 70 robotics educators from across the country in 4 robotics certification courses alongside CMU professor

INVOLVEMENT AND LEADERSHIP:

Casualty Actuary Society University Ambassador, State College, PA *Aug 2017 – Present*

- Coordinate on-site presentations by CAS insurance professionals to increase student awareness of the CAS track
- Organized Penn State's first Actuarial Case Study where 50 students competed for cash prizes worth over \$5,000

Actuarial Science Club, State College, PA *Aug 2015 – Present*

- Apply information from corporate workshops and personal experiences to participate in club mentoring program

The Village Retirement Community Band, State College, PA *Aug 2016 – Present*

- Volunteered at the Penn State Village assisted living facility as a drummer for Honors College service group
- Entertained residents with both nostalgic and modern musical performances and dinner discussions

First Lego League Robotics Team Coach, Pittsburgh, PA *Sep 2011 – Feb 2016*

- Coached over 10 youth robotics teams in 6 FLL competitions, winning the 2016 Western PA Regional Tournament

Academic Vita

PUBLICATIONS:

Geospatial-Risk-Based Recoupment for TRIA Eligible Insurance,
Journal of Risk and Insurance
Collaborators: Zhongyi Yuan

Apr 2019

Sensor-Enabled Clawbot Construction,
Carnegie Mellon Robotics Academy
Collaborators: Robin Shoop, Jesse Flot, Vu Nguyen

Aug 2013

TECHNICAL EXPERTISE:

Computer Languages: R, VBA, SQL, SAS, Python (Workplace Experience)
Mechanical Design: AutoDesk Inventor, AutoCAD (Workplace Experience)
Other Programs: MS Excel, MS Word, MS PowerPoint, LaTeX (Proficient)
Languages: English (Fluent), Brazilian-Portuguese (Native)

AWARDS:

President's Freshman Award: Awarded for completing 1 semester with 4.0 GPA *Jan 2016*
President's Sparks Award: Awarded for completing 3 semesters with 4.0 GPA *Jan 2017*
Evan Pugh Junior/Senior Award: Awarded for completing 5 semesters in the top 0.5% of my class *Jan 2018*
DW Simpson Scholarship: Awarded to 4 rising seniors in the Actuarial Science major *Feb 2018*
CAMAR Actuarial Scholarship: Awarded to rising seniors in the Actuarial Science major *May 2018*